U-Pb dating of middle Eocene-Pliocene multiple tectonic pulses in the Alpine foreland

Luca Smeraglia[1,2,3], Nathan Looser[4*], Olivier Fabbri[2], Flavien Choulet[2], Marcel Guillong[4], Stefano M. Bernasconi[4]

1. National Research Council, IGAG, Rome, Italy
2. Chrono-Environnement, UMR 6249, Université de Bourgogne-Franche Comté, 25000 Besançon, France
3. formerly at Dipartimento di Scienze della Terra, Sapienza Università di Roma, P.le Aldo Moro 5, 00185, Roma
4. Geological Institute, ETH Zürich, Sonneggstrasse 5, 8092 Zürich, Switzerland

*Corresponding author e-mail address: Nathan.looser@erdw.ethz.ch

Abstract. Foreland fold-and-thrust belts record long-lived tectono-sedimentary activity, from passive margin sedimentation, flexuring, and further involvement into wedge accretion ahead of an advancing orogen. Therefore, dating fault activity is fundamental for plate movement reconstruction, resource exploration or earthquake hazard assessment. Here, we report U-Pb ages of syntectonic calcite mineralizations from four thrusts and three tear faults sampled at the regional scale, across the Jura fold-and-thrust belt in the northwestern Alpine foreland (eastern France). Three regional tectonic phases are recognized in the middle Eocene-Pliocene interval: (1) pre-orogenic faulting at 48.4 ± 1.5 and 44.7 ± 2.6 Ma associated to the far-field effect of the Alpine compression, (2) syn-orogenic thrusting at 11.4 ± 1.1, 10.6 ± 0.5, 9.7 ± 1.4, 9.6 ± 0.3, and 7.5 ± 1.1 Ma associated to the formation of the Jura fold-and-thrust belt with possible in-sequence thrust propagation, and (3) syn-orogenic tear faulting at 10.5 ± 0.4, 9.1 ± 6.5, 5.7 ± 4.7, and at 4.8 ± 1.7 Ma including the reactivation of a pre-orogenic fault at 3.9 ± 2.9 Ma. Previously unknown faulting events at 48.4 ± 1.5 and 44.7 ± 2.6 Ma predate by ~10 Ma the reported late Eocene age for tectonic activity onset in the Alpine foreland. In

addition, we dated the previously inferred re-activation of pre-orogenic strike-slip faults as tear faults during Jura imbrication. The U-Pb ages document a minimal time frame for the evolution of the Jura FTB wedge by possible in-sequence thrust imbrication above the low-friction basal décollement consisting of evaporites.

1. Introduction

Foreland fold-and-thrust belts develop at the external edges of orogens and are characterized by a multiphase tectono-sedimentary history including: pre-orogenic sedimentation, uplift at the peripheral bulge of the advancing orogen, progressively accelerating subsidence followed by syn-tectonic sedimentation, and accretion of the sedimentary cover into the foreland fold-and-thrust belt (Lacombe et al., 2007). Unraveling the timing of these tectonic events is fundamental for plate kinematic modelling, natural resource exploration, paleoseismicity, and topography evolution studies (Vergés et al., 1992; Craig and Warvakai, 2009). However, deciphering the different tectonic phases is complicated by the overprinting of inherited structures by progressively younger tectonic events.

This issue is addressed by dating syn-tectonic sediments and, more recently, better constrained through dating of fault activity with K-Ar, $^{40}Ar/^{39}Ar$, and U-Pb and U-Th methods (Van der Pluijm et al., 2009; Vrolijk et al., 2018). In particular, calcite U-Pb and U-Th geochronology (Roberts et al., 2020) is the unique method for dating syntectonic calcite mineralizations. This technique has been applied for dating single faults in extensional, strike-slip, and compressional settings (Goodfellow et al., 2017; Nuriel et al., 2017; Hansman et al., 2018; Smeraglia et al., 2019; Carminati et al., 2020). So far, the dating of multiple faults at the regional scale across a foreland fold-and-thrust belt remains rare (Beaudoin et al., 2018; Looser et al., 2021).

In this study, we dated syntectonic calcite mineralizations from four thrusts and three tear faults sampled across the Jura fold-and-thrust belt (Jura FTB, eastern France, Fig. 1) by laser ablation inductively coupled plasma mass spectrometry (LA-ICP-MS) U-Pb dating. We reconstructed three tectonic phases having occurred in the middle Eocene-Pliocene period, documenting a long-lived

polyphase tectonic history of the northwestern Alpine foreland system along the convergent boundary between European and African plates.

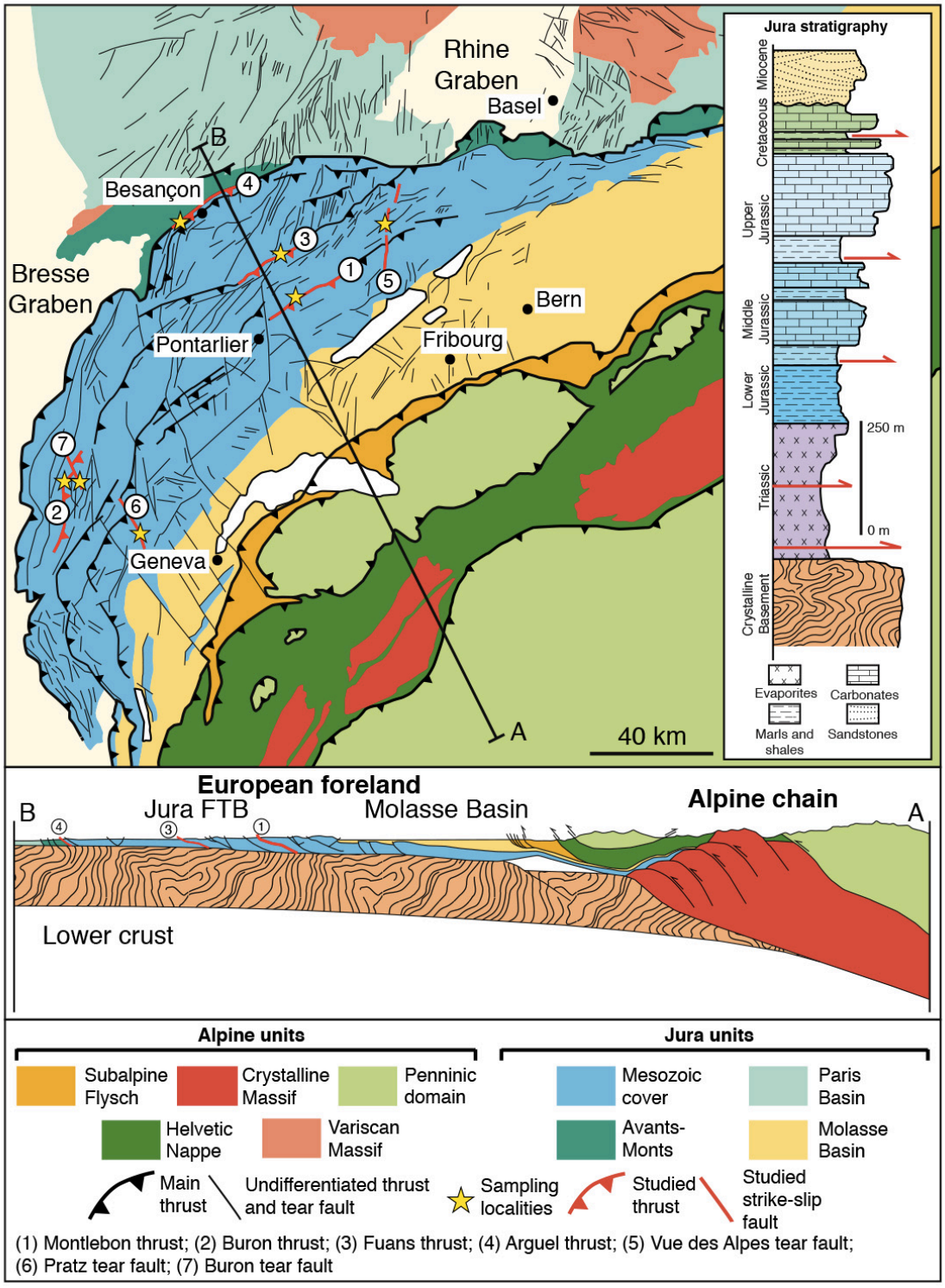

Figure 1. Geological map of the northwestern Alpine foreland and surrounding areas and stratigraphic column of the main lithological units of the Jura area. Modified from Rime et al. (2019).

2. Tectonic setting

The Jura FTB is located in the foreland of the Western Alps and formed by the ongoing continental collision of the Eurasian plate with the African plate (Sommaruga, 1997; Mosar, 1999; Lacombe and Mouthereau, 2002; Affolter and Gratier 2004; Bellahsen et al., 2014) (Fig. 1). Shortening affected the Triassic-late Miocene sedimentary succession deposited on the European passive margin above the Hercynian crystalline basement and caused brittle-ductile deformation at several levels (Fig. 1) (Philippe et al., 1996; Homberg et al., 2002; Ustaszewski and Schmid, 2006). The sedimentary succession starts with Triassic shales and evaporites overlain by Jurassic-Cretaceous shales, marls, and limestones (Fig. 1) (Sommaruga et al., 2017). Following a Late Cretaceous-Eocene regional unconformity, Oligocene-Miocene shallow marine to continental clastic deposits of the Molasse Basin were deposited above Cretaceous limestones (Fig. 1).

The post-Mesozoic tectonic history of the Jura area is assumed to have started in the middle Eocene with N-S shortening related to the far field effect of the "Pyrenean orogeny" generating strike-slip faults (Bergerat, 1987). However, no absolute ages of this tectonic phase are available. Based on structural analyses and calcite U-Pb ages, two phases of normal faulting during the Late Eocene and Oligocene in the distal parts of the Molasse Basin in northern Switzerland have been documented. Normal faulting during the Late Eocene has been related to crustal extension due to the opening of the Rhine Graben, while normal faulting during the middle Miocene has been related to crustal tilting associated to uplift of the Black Forest Highlands and subsidence of the northern part of the Molasse Basin (Mazurek et al., 2018).

Biostratigraphic dating of syn-orogenic deposits, geomorphological observations, interpretation of seismic reflection profiles, and syntectonic calcite U-Pb ages of fault activity in the eastern tip of Jura FTB indicate that orogenic shortening started ~14.5 Ma ago (Langhian times) at the latest (Looser et al., 2021 and references therein) and is still active (Mosar, 1999; Becker, 2000; Madritsch et al., 2008). Shortening was accomodated by N to NE-verging and NE-SW-striking thrusts and by NW-SE to N-S trending sinistral tear faults (Sommaruga, 1997) (Fig. 1). The main

décollement level of the thrust system developed along Triassic evaporites (Jordan, 1992; Pfiffner, 2014; Gruber, 2017; Sommaruga et al., 2017). Therefore, there is a common agreement in considering the Jura FTB mainly as the product of thin-skinned tectonics (Sommaruga, 1997). However, thick-skinned tectonics occurred in the late stage of deformation and only in the external part (Ustaszewski and Schmid, 2006, 2007; Madritsch et al., 2008; Lacombe and Bellahsen, 2016).

Field cross-cutting relationships and U-Pb ages of syntectonic calcite mineralizations show that tear faults were synchronously active with thrusting and folding (Sommaruga, 1997; Looser et al., 2021) and their movement continued after thrusting. In fact, in some cases, tear faults are still seismogenic (Thouvenot et al., 1998). Several authors suggested that pre-orogenic strike-slip and normal faults were reactivated in early Pliocene, respectively as tear and transpressional faults (Madritsch et al., 2008; Homberg et al., 1997; Ustaszewski and Schmid, 2006). Overall, no direct dating of this fault re-activation has been available up to date.

3. Methods

The following methods were used: (1) field structural analyses and vein/slickenfiber sampling from four major thrusts (From SE to NW: Montlebon, Buron, Fuans, and Arguel thrusts) and three NNE-SSW tear faults (Vue des Alpes, Pratz, and Buron) moving from the internal (most deformed) to the external (less deformed) parts of the Jura FTB (Fig. 1). In particular, we measured the orientation of sampled veins and the rake of sampled slickenfibers in order to combine U-Pb ages from veins and slickenfibers with structural measurements; (2) microstructural analyses with optical microscope and cathodoluminescence to unravel different phases of calcite precipitation; (3) calcite U-Pb LA-ICP-MS dating on veins and slickenfibers to date fault activity. In most cases, the U-Pb analyses were performed on calcite crystals showing a homogenous color or undisturbed growth-zoning under cathodoluminescence light, indicating no open-system alteration after calcite precipitation by late fluid infiltration and/or recrystallization (Figs. S1-S3). As commonly done in LA-ICP-MS U–Pb carbonate dating, no disequilibrium correction for initial $^{234}U/^{238}U$ and ^{230}Th was

111 applied. This may cause underestimation of young (<10 Ma) samples (Roberts et al., 2020).
112 Analytical details are described in the Supplementary Material.
113
114 **4. Results**
115 *4.1 Structural and microstructural observations*
116 The Montlebon, Buron, Fuans, and Arguel thrusts are NNE- to SW-NE striking and N- to NW-
117 verging thrusts (Madritsch et al., 2008; Rime et al., 2019; Smeraglia et al., 2020) (Fig. 2a-d). In
118 particular, the Montlebon thrust is characterized by E to ESE-dipping (30-90°) thrust planes with
119 slickenfibers showing left-lateral transpressional movements with N to NNW tectonic transport
120 directions (Fig. 2a). The Buron thrust is characterized by E to SE-dipping (20°-30°) thrust planes with
121 slickenfibers showing left-lateral transpressional movements with NW tectonic transport directions
122 (Fig. 2b). The Fuans thrust is characterized by E to SE-dipping (20°-40°) thrust planes with
123 slickenfibers showing left-lateral transpressional movements with NNW to NW tectonic transport
124 directions (Fig. 2c). The Arguel thrust is characterized by S-dipping (10-30°) thrust planes with
125 slickenfibers showing right-lateral transpressional movements with NNW tectonic transport
126 directions (Fig. 2d).
127 The subvertical Vue des Alpes, Pratz, and Buron tear faults show a sinistral strike-slip
128 displacement (Sommaruga, 1997) (Fig. 2de-g). In particular, the Vue des Alpes strike-slip fault is
129 characterized by NE-SW-striking subvertical fault planes with slickenfibers showing sinistral
130 movements and associated NW-SE-striking subvertical fault planes with slickenfibers showing
131 dextral movements (Fig. 2e). Both the Pratz and Buron strike-slip faults are characterized by NE-SW-
132 striking subvertical fault planes with slickenfibers showing sinistral movements (Fig. 2f-g).

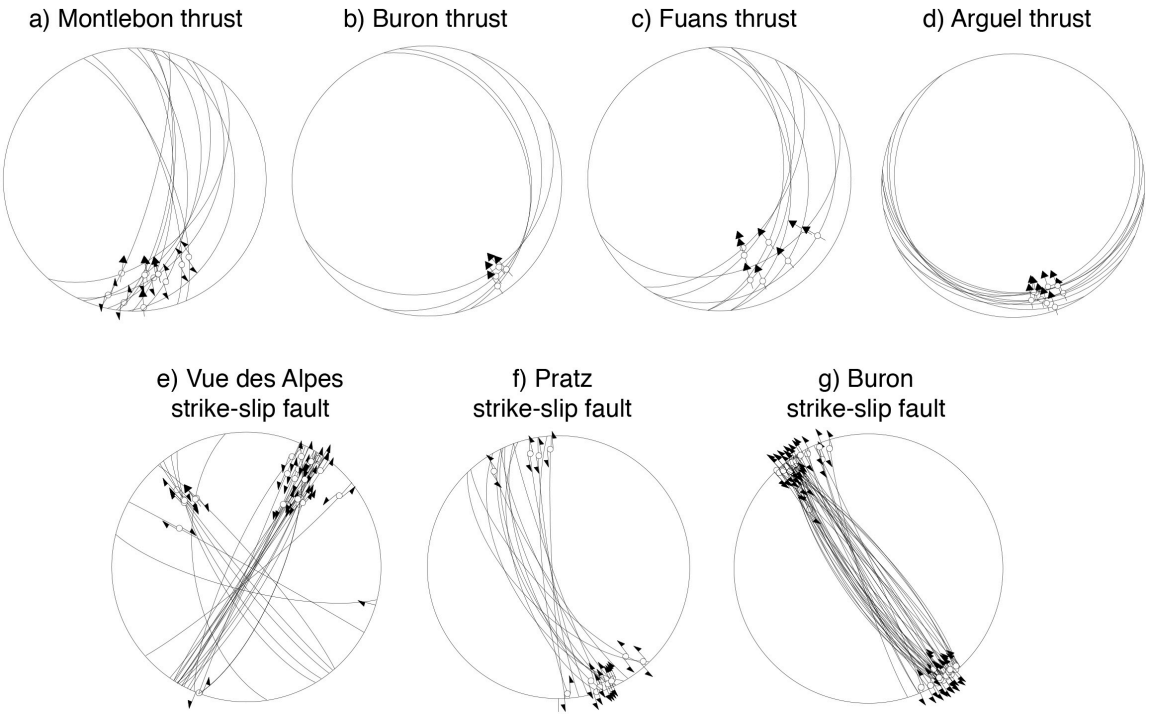

Figure 2. Lower Schmidt hemisphere projection of fault-slip data and slip vectors for thrust and strike-slip faults. **(a)** Montlebon thrust. **(b)** Buron thrust. **(c)** Fuans thrust. **(d)** Arguel thrust. **(e)** Vue des Alpes strike-slip fault. **(f)** Pratz strike-slip fault. **(g)** Buron strike-slip fault-

Both thrusts and strike-slip faults cut through Middle-Upper Jurassic and Lower Cretaceous limestones. The fault core zones are characterized by foliated fault rocks cut by sharp fault planes (Fig. 3a-d). Breccia lenses are developed in the Buron thrust core (Fig. 4d). Calcite mineralizations in extensional veins (Buron, Arguel, Montlebon, Vue des Alpes, and Pratz) and in slickenfibers (Fuans, Vue des Alpes, and Pratz) were sampled.

Extensional veins occur in limestone fragments of foliated fault rocks (Fig. 3e,g) and in clasts from breccias (Figs. 3f and 4g). In limestone fragments of foliated fault rocks, extensional veins are oriented perpendicularly to stylolites (Fig. 3e,g), which occur along S- and C-planes. Extensional veins in clasts from breccias show a crackle-like texture and mutually cross-cutting relationships (Fig. 3f). Extensional veins are filled by blocky to elongated-blocky calcite crystals and show syntaxial growth (Figs. 3i-k, 4g, S1a-d, S2a,b,g,h, S3a-h).

The fault planes are coated by slickenfibers (Figs. 3d,h and 4e,f). At the microscale, slickenfibers occur in dilational jogs along shear planes (Fig. 3h) and are filled by fibrous calcite crystals bounded by sharp shear planes (Figs. 3j, 4i, S1e-h, and S2c-f) and/or by blocky calcite crystals (Figs. 3l and 4h). Fibrous crystals are oriented parallel to shear planes.

Most of the studied veins and slickenfibers show homogeneous cathodoluminescence colors, ranging from bright to dull red, and/or show cathodoluminescence zoning on the same crystal (Figs. 3i-l, 4g-i, S1a,c,e,g, S2a,c,e,g, and S3a,c,e,g). In places, slickenfibers and extensional veins are cross-cut by extensional veins showing black to dull red luminescence colors (Figs. S1e-h, S2c-f, and S3a,b,g,h)

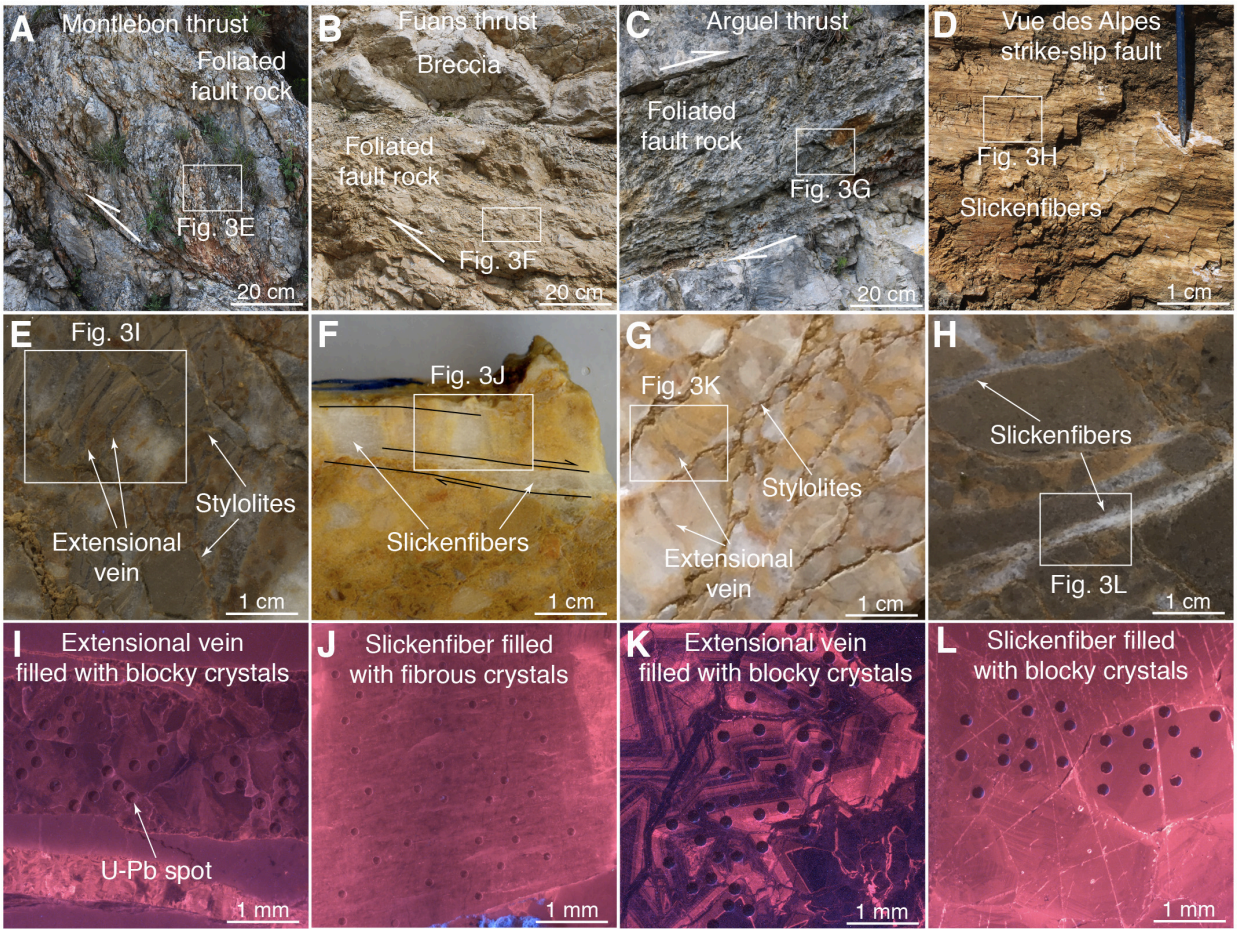

Figure 3. Foliated fault rocks in the fault core of the Montlebon thrust **(a)**, Arguel thrust **(b)**, and **(c)** Fuans thrust. **(d)** Detail of minor fault plane along the Vue des Alpes strike-slip fault showing calcite slickenfibers. **(e)** Hand sample from the Montlebon thrust showing host rock sigmoids bounded by stylolites and extensional veins perpendicular to stylolites. **(f)** Hand sample from the Fuans thrust showing host rock sigmoids bounded by stylolites and extensional veins

perpendicular to stylolites. **(g)** Hand sample from the Arguel thrust showing extensional veins with crackle-like texture. **(h)** Hand sample from a minor fault plane along the Vue des Alpes strike-slip fault showing slickenfibers developed along dissolution planes. **(i-l)** Cathodoluminescence microphotographs of thin sections showing extensional veins and slickenfibers from the studied faults with ablation craters of the U-Pb analyses.

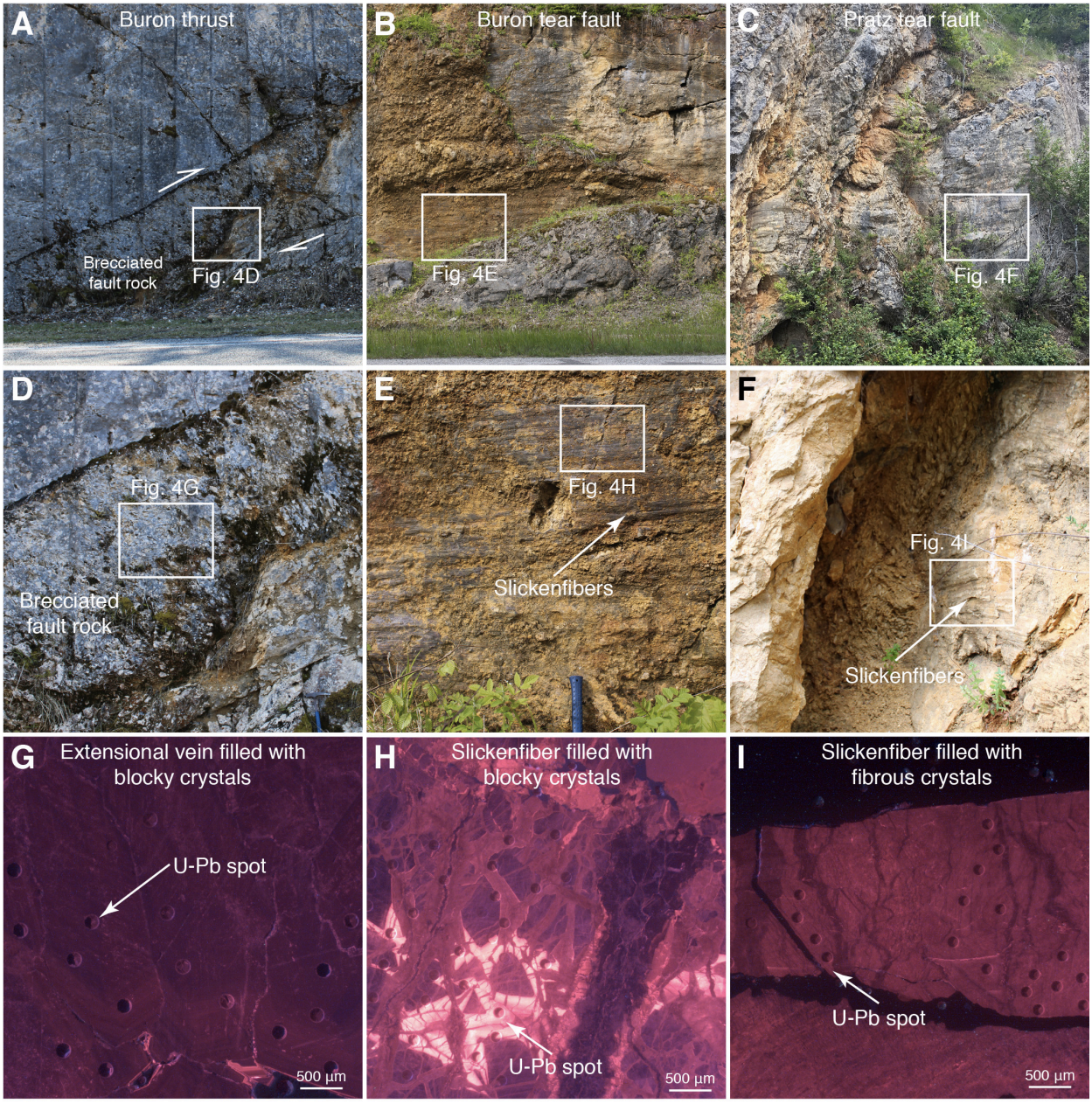

Figure 4. **(a)** Buron thrust. **(b)** Buron tear fault. **(c)** Pratz tear fault. **(d)** Brecciated fault rocks in the fault core of the Buron thrust. **(e)** Brecciated fault rocks cut by sharp fault planes in the fault core of the Buron tear fault. **(f)** Foliated fault rock cut by sharp fault planes in the fault core of the Pratz tear fault. **(g-i)** Cathodoluminescence microphotographs of

thin sections showing extensional veins and slickenfibers from the studied faults with ablation craters of the U-Pb analyses.

4. 2 U-Pb dating

A total of 12 reliable lower intercept ages (Figs. 5 and 6) out of 19 analyses (rejected age data is presented in Fig. S4) are reported with uncertainties at 2σ absolute including counting statistics uncertainties, uncertainty of the primary reference material and inter-session variations (Guillong et al., 2020). The U-Pb ages indicate different phases of tectonic activity and related calcite precipitation in the middle Eocene to Pliocene period and also multiple precipitation ages along the same fault (Supplementary Information Table 1).

An extensional vein from the Montlebon thrust shows a Serravallian age of 11.4 ± 1.1 Ma (Fig. 5a). An extensional vein from the Buron thrust shows a Tortonian age of 10.6 ± 0.5 Ma (Fig. 5b). Two slickenfibers from the Fuans thrust yield Tortonian ages indistinguishable from each other of 9.7 ± 1.4 Ma and 9.6 ± 0.3, respectively (Fig. 5c,d). An extensional vein from the Arguel thrust shows a Tortonian-Messinian age of 7.5 ± 1.1 Ma (Fig. 5e). Along the Vue des Alpes strike-slip fault, two slickenfibers yield Ypresian-Lutetian ages of 44.7 ± 2.6 and 48.4 ± 1.5 Ma (Fig. 6a,b), while an extensional vein shows a Pliocene age of 3.9 ± 2.9 Ma (Fig. 6c). An extensional vein from the Buron strike-slip fault shows a Messinian age of 5.7 ± 4.7 Ma (Fig. 6d). One slickenfiber and one extensional vein from the Pratz strike-slip fault show Tortonian-Messinian ages of 10.5 ± 0.4 and 9.1 ± 6.5 Ma (Fig. 6f-g), while one slickenfiber shows a younger age of 4.8 ± 1.7 Ma (Fig. 6e). Because of the common-lead rich $^{207}Pb/^{206}Pb$ compositions, the U-Pb ages of the samples DA2, BUS1, PR1-A, PR2-2 of the strike-slip faults have larger uncertainties than those of the thrusts.

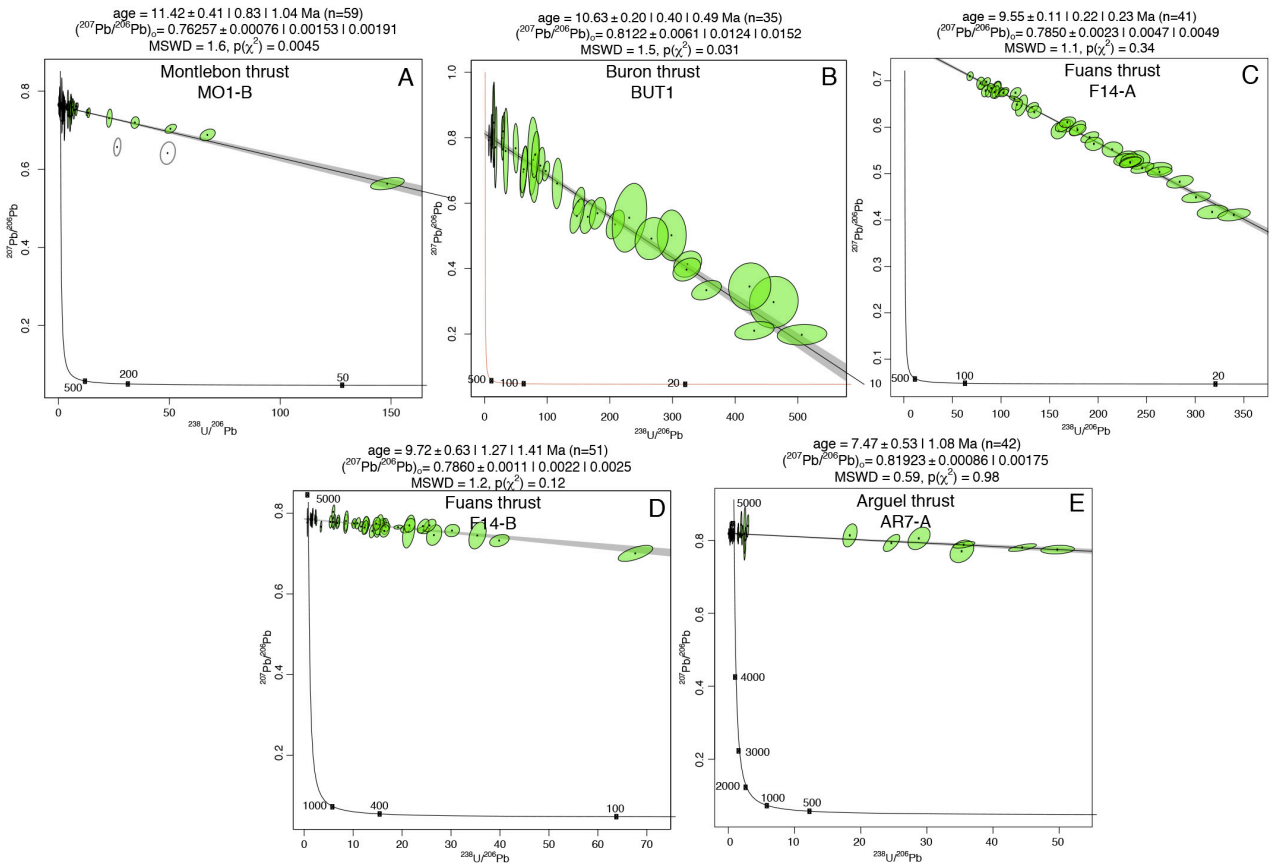

196

197 **Figure 5.** Tera-Wasserburg concordia diagrams of thrust faults. **(a)** Montlebon thrust. **(a)** Buron thrust. **(c,d)** Fuans thrust.

198 **(e)** Arguel thrust.

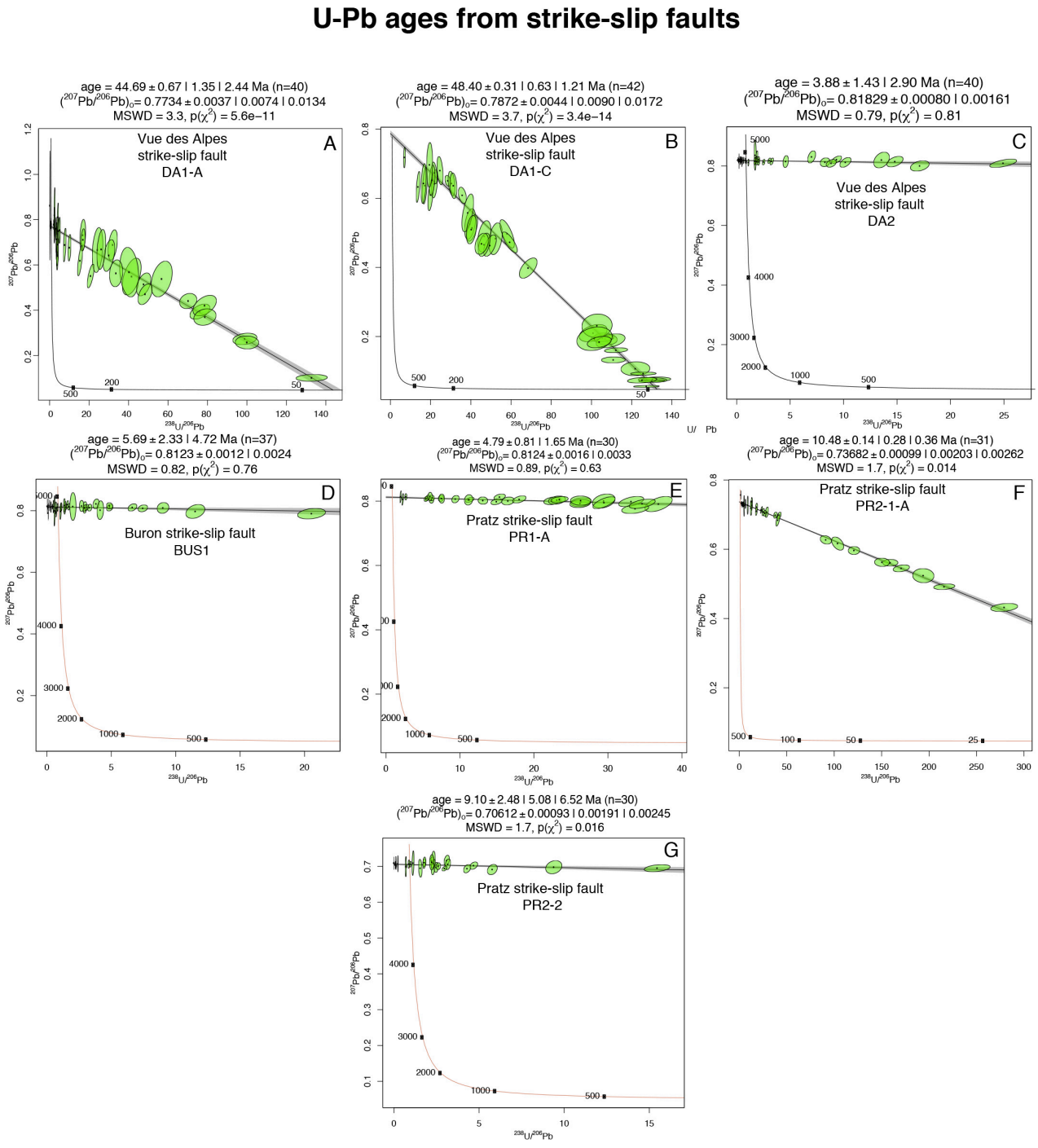

Figure 6. Tera-Wasserburg concordia diagrams of strike-slip faults. **(a-c)** Vue des Alpes strike-slip fault. **(d)** Buron strike-slip fault. **(e-g)** Pratz strike-slip fault.

5. Discussion and conclusions

205 Slickenfibers on sharp fault planes are clear evidence of tectonic slip along faults (Figs. 3j-l, 4i,
206 S1e-h, and S2c,f). In particular, blocky and fibrous crystals indicate respectively fast and slow vein
207 opening rates associated with fault slip. Within slickenfibers, calcite crystal precipitated during syn-
208 to early post-slip fluid influx in newly formed dilational sites formed along undulated and sharp slip
209 planes (Gratier and Gamond, 1990; Urai et al., 1991; Holland and Urai, 2010; Fagereng et al., 2010;
210 Bons et al., 2012; Woodcock et al., 2014). Extensional veins oriented perpendicular to stylolites (Fig.
211 3e,g) are linked to syn-thrusting shortening (Gratier et al., 2013). The studied veins are therefore
212 interpreted as the product of tectonic fault slip and their U-Pb ages are considered as representative
213 of faulting activity.
214 We recognize three regional tectonic phases between the middle Eocene and the Pliocene (Figs.
215 7 and 8) which are linked to the long-lived tectonic activity of the Alpine foreland evolution. The
216 presented ages should be regarded as minimum ages for the onset of deformation at the studied faults
217 or as maximum ages for its termination as potentially older or younger deformation phases recorded
218 by other veins and slickenfibers not sampled and analyzed here may have been missed.
219 The U-Pb ages are regionally consistent in terms of tectonic evolution of the Jura FTB and the
220 microstructures of the analyzed veins and slickenfibers indicate precipitation during syn- to early
221 post-slip fluid influx. However, although U-Pb dating was performed on crystals with no indication
222 of later open-system alteration based on CL-microscopy, possible late fluid infiltration and calcite
223 recrystallization cannot be excluded as previously suggested by other studies (Beaudoin et al., 2018;
224 Hoareau et al., 2021; Roberts et al., 2020, 2021).
225 Sample BUS1 clearly shows multiple calcite phases indicating vein re-opening and potentially
226 different ages (Fig. 4h). However, the Tera-Wasserburg diagram of BUS1 shows a single age trend
227 with a low MSWD of 0.82 (Fig. 6d). This would not be observed in a sample that experienced
228 crystallization at significantly different times. Therefore, sample BUS1 reflects calcite precipitation
229 within a time interval smaller than what would result in multiple age trends.

The oldest tectonic phase is recorded by two horizontal slickenfibers dated at 44.7 ± 2.6 and 48.4 ± 1.5 Ma in Ypresian-Lutetian times (middle Eocene) along the Vue des Alpes strike-slip fault (Fig. 7). These ages are ~10 Ma older than the onset of the extensional tectonic activity in Priabonian (late Eocene) related to Rhine Graben opening (Sissingh, 1998; Mazurek et al. 2018). The strike-slip faulting in Eocene times is consistent with fault-slip data of Homberg et al. (1997). We propose that the Ypresian-Lutetian tectonic activity can be related to the late Mesozoic-Eocene far field tectonic shortening in the European plate foreland due to the advancing Alpine orogen (Mazurek et al., 2006; Timar-Geng et al., 2006) (Fig. 8a). On the contrary, previous studies suggested that middle Eocene strike-slip faulting in the Jura area was related to the far-field effect of the Pyrenean compression (Bergerat, 1987; Homberg et al., 2002). The Pyrenean far field effect has also been recognized in the Paris Basin (eg, Lacombe et al., 1990; Lacombe and Mouthereau, 1999; Lacombe and Obert, 2000), in eastern France (Lacombe et al., 1993), and even in the UK (Hibsch et al., 1995) where Pyrenean-related calcite veins were dated by U-Pb (Parrish et al., 2018). However, even though tectonic stresses have been shown to be transmitted more than thousand km away from the orogenic front (Craddock et al., 1993; Beaudoin and Lacombe, 2018), further studies are necessary to better constrain the origin of pre-Miocene fault activity in the European foreland.

Structural analyses of the studied thrusts highlight N to NW oriented tectonic transport directions (Fig. 4a-d) consistent with the regional NW-SE to N-S compressional phase that has affected the Jura fold and thrust belt since the Miocene (Philippe et al, 1996; Becker, 2000; Homberg et al., 2002; Ustaszewski and Schmid, 2006; Madritsch et al., 2008; Looser et al., 2021). Although age uncertainties do not allow a distinction beyond doubt and the limited numbers of U-Pb ages and studied thrusts provide a limited picture, the Jura imbrication seems to have occurred by in-sequence thrusting. The oldest observed thrusts ages are Serravallian-Messinian and become progressively younger moving from the inner (SE) toward the external (NW) part, from 11.4 ± 1.1, 10.6 ± 0.5, 9.7 ± 1.4 and 9.6 ± 0.3 on the same thrust, and 7.5 ± 1.1 Ma, respectively, in the Montlebon, Buron, Fuans, and Arguel thrusts (Figs. 7 and 8b). These ages are consistent with the time interval of ~14.5-

256 3.3 Ma suggested for thrusting activity from biostratigraphic dating of syn- to post-tectonic sediments
257 (Becker, 2000 and references therein) and from calcite U-Pb ages of thrust activity in the eastern Jura
258 FTB (Looser et al., 2021) (Fig. 7).

259 Previous studies interpreted the subvertical strike-slip faults in the Jura FTB as tear faults, with
260 activity during thrusting and folding (Sommaruga, 1997; Looser et al., 2021). Our structural analyses
261 and U-Pb ages from the studied strike-slip faults support this interpretation. In particular, strike-slip
262 faults are subvertical and are roughly parallel or oblique to the regional transport directions inferred
263 from thrust kinematics (compare tectonic transport directions of Fig. 4a-d with those of Fig. 4f,g), a
264 common feature of tear faults (Twiss and Moores, 1992).

265 The Buron thrust, active at 10.6 ± 0.5 Ma, was cross-cut by the Buron tear fault ~5 Ma later, at
266 5.7 ± 4.7 Ma (Figs. 7 and 8c). The Pratz tear fault was active at 10.5 ± 0.4 and 9.1 ± 6.5 Ma, indicating
267 tear faulting generation during coeval thrust propagation, and further late-orogenic re-activation at
268 4.8 ± 1.7 Ma (Figs. 7 and 8b). These data indicate that tear faulting occurred during syn- to late-
269 orogenic times (Fig. 8b,c). In addition, a late-orogenic phase is recorded by an extensional vein from
270 the Vue des Alpes strike-slip fault showing a Pliocene age of 3.9 ± 2.9 Ma (Fig. 7). This age has been
271 measured on an extensional vein that cannot be directly related to fault slip. Therefore, we cannot
272 completely exclude that this age represents a late alteration event not directly linked to fault slip
273 during the Pliocene. However, the 3.9 ± 2.9 Ma age is consistent with late orogenic deformation
274 between 4.2 and 2.9 Ma documented in the frontal part of the Jura FTB (Madritsch et al., 2008 and
275 references therein). The 3.9 ± 2.9 Ma age from the Vue des Alpes strike-slip fault is ~40 Ma younger
276 than the middle Eocene ages (44.7 ± 2.6 and 48.4 ± 1.5 Ma) measured on the same fault, suggesting
277 the reactivation of the Vue des Alpes strike-slip fault during late Jura shortening. This inference is
278 also consistent with field cross-cutting relationships indicating re-activation of pre-existing strike-
279 slip faults as tear faults (Homberg et al., 1997).

280 We consider the retrieved age as fault re-activation of the Vue des Alpes strike-slip fault and
281 relate it to a stress change from pure compression to strike-slip state of stress coupled with the

occurrence of an inherited strike-slip fault favorably oriented with respect to the regional stress field. This stress change associated with tear fault development can be related to progressive fold-and-thrust belt thickening and erosion initiating only after ~4.5 Ma (Looser et al., 2021 and references therein), which led to an increase in the maximum vertical stress (sigma 3) and a switch between sigma 3 and 2 (Ferril et al., 2021). Shortening is still active in the Jura FTB and tear faults (also re-activated tear faults) are seismogenic (Thouvenot et al., 1998).

The presented tectonic reconstruction depicts a stable evolution of the Jura FTB wedge by possible in-sequence thrusting consistent with thrust imbrication above the low-friction décollement consisting of evaporites (Fig. 8a-c). Contrarily, out-of-sequence thrusting occurred as late as in Messinian-early Pliocene times in the proximal Molasse Basin (Von Hagke et al., 2012, 2014) and in the Alps (Bellahsen et al., 2014). This tectonic framework suggests a stable topographic evolution of the critical taper and topographic profile of the Jura fold-and-thrust belt. Finally, this study constrains a long-lived polyphase tectonic history of the northwestern Alpine foreland system along the convergent boundary between European and African plates from the middle Eocene to the Pliocene.

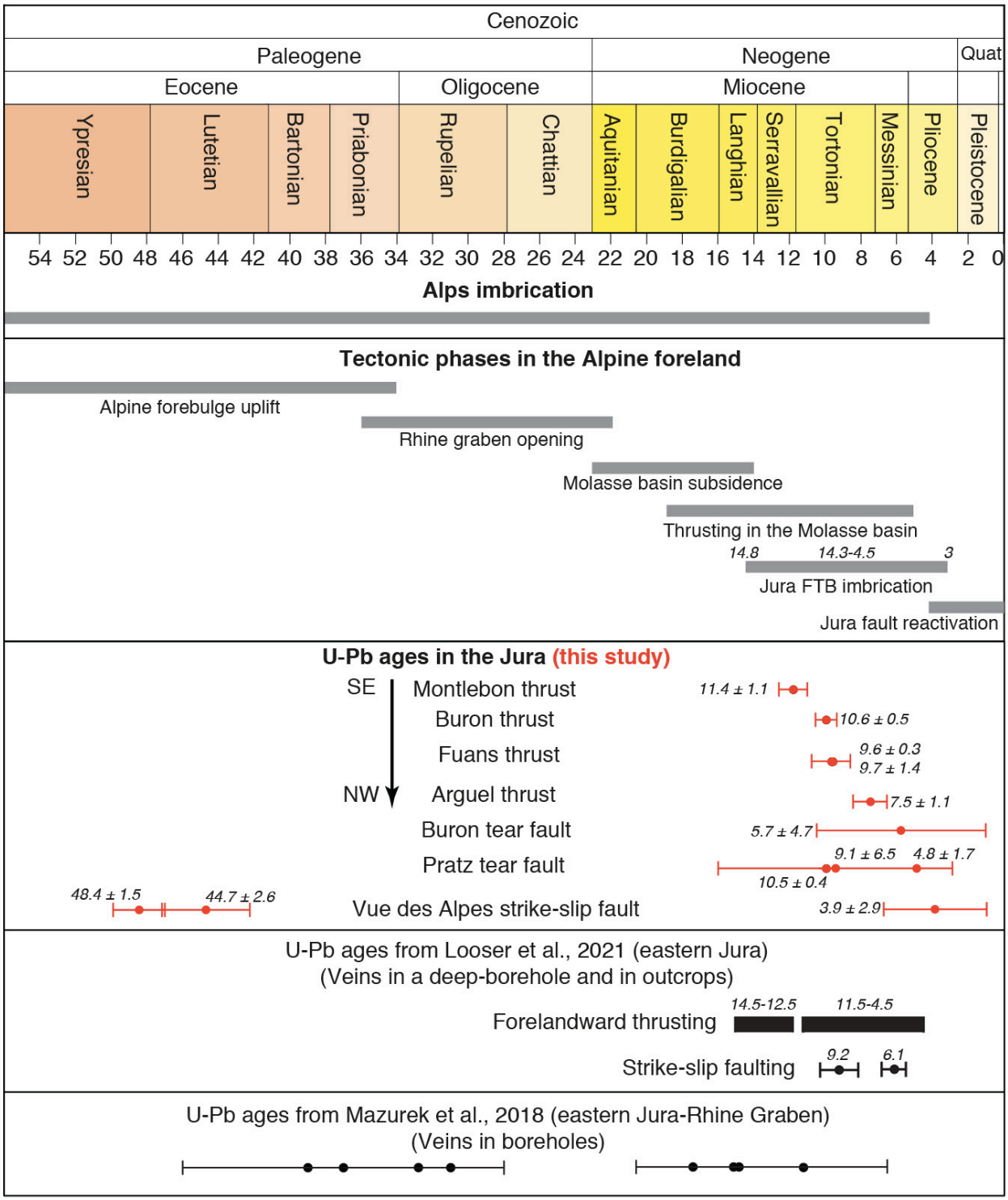

Figure 7. Main tectonic phases in the Alps and in the Alpine foreland. Age constraints shown as grey bars are from Burkhard and Sommaruga (1998), Ustaszewski et al. (2006), Madritsch et al. (2008), Bellahsen et al. (2014), and Von Hagke et al. (2014). For calcite U-Pb data, all uncertainties are represented as 2σ.

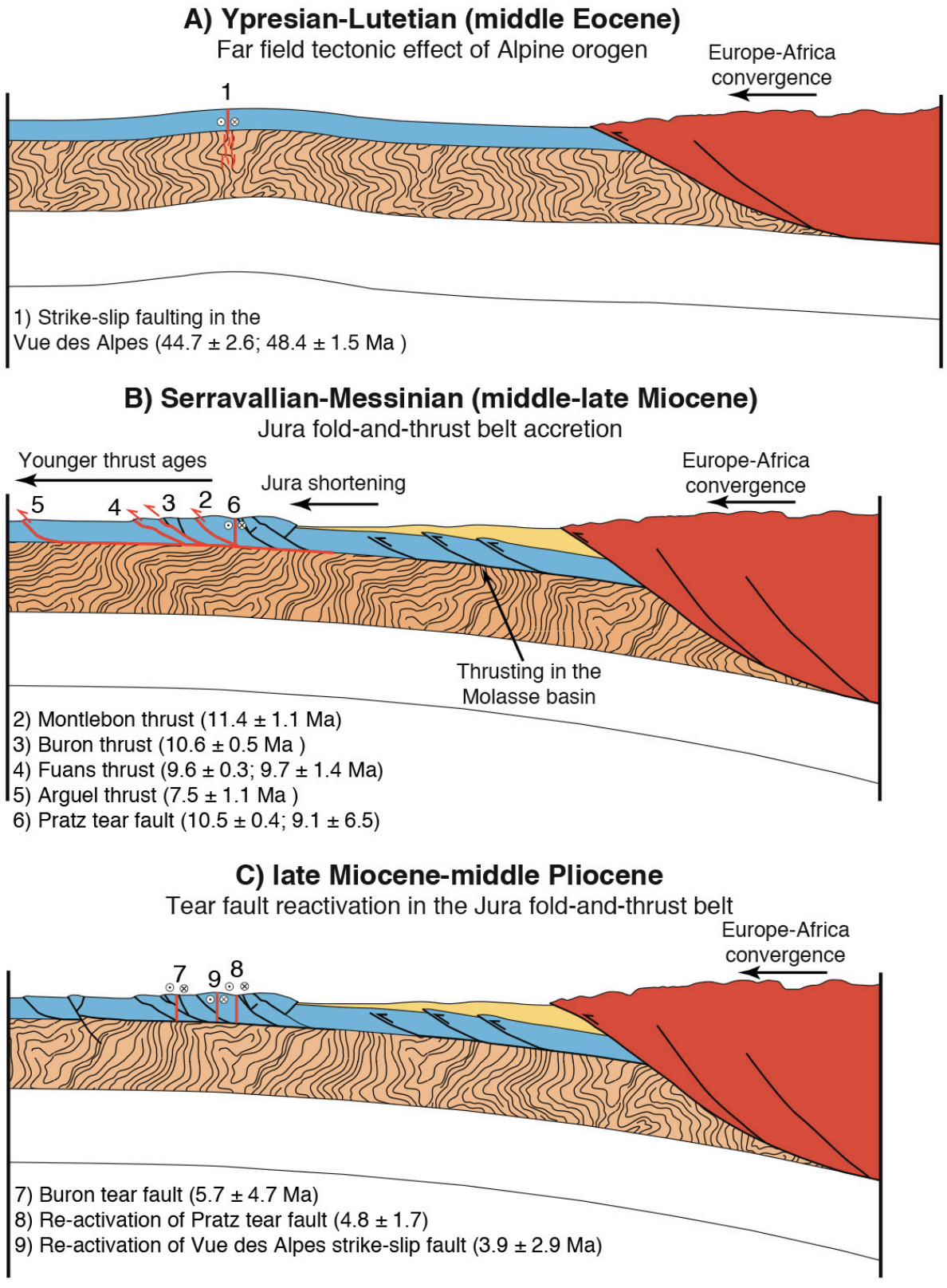

300

301 **Figure 8. (a-d)** Schematic reconstruction of the main tectonic phases dated in the Jura area in the regional context of the

302 Alpine foreland system evolution.

ACKNOWLEDGEMENT

We thank CASP (https://www.casp.org.uk/) for financial support during fieldwork activity by the Andy Whitham Fieldwork Award 2019 to L. Smeraglia. Financial support by Borsa di Perfezionamento Estero 2017 (Sapienza) to L. Smeraglia, UMR 6249 and OSU Theta projects to O. Fabbri and F. Choulet are acknowledged. U-Pb analyses were funded by the Swiss National Science Foundation project number 200021_169849 to S. M. Bernasconi. We thank J. Mosar, M. Schori, A. Sommaruga, C. Mottran, L. Weiss, and C. Von Hagke for constructive discussions and suggestions, also during fieldwork. We thank the Editor Susanne Buiter and two Reviewers Olivier Lacombe and Nick Roberts for their constructive comments that helped to improve the manuscript.

REFERENCES

Affolter, T., and Gratier, J. P.: Map view retrodeformation of an arcuate fold-and-thrust belt: The Jura case. Journal of Geophysical Research: Solid Earth, 109(B3), 2004.

Beaudoin, N., and Lacombe, O.: Recent and future trends in paleopiezometry in the diagenetic domain: Insights into the tectonic paleostress and burial depth history of fold-and-thrust belts and sedimentary basins. Journal of Structural Geology, 114, 357-365, 2018.

Beaudoin, N., Leprêtre, R., Bellahsen, N., Lacombe, O., Amrouch, K., Callot, J. P., ... and Daniel, J. M.: Structural and microstructural evolution of the Rattlesnake Mountain Anticline (Wyoming, USA): new insights into the Sevier and Laramide orogenic stress build-up in the Bighorn Basin. Tectonophysics, 576, 20-45, 2012.

Beaudoin, N., Lacombe, O., Roberts, N. M., and Koehn, D.: U-Pb dating of calcite veins reveals complex stress evolution and thrust sequence in the Bighorn Basin, Wyoming, USA. Geology, 46(11), 1015-1018, 2018.

Becker, A.: The Jura Mountains - an active foreland fold-and-thrust belt?. Tectonophysics, 321(4), 381-406, 2000.

329 Bellahsen, N., Mouthereau, F., Boutoux, A., Bellanger, M., Lacombe, O., Jolivet, L., and Rolland,
330 Y. : Collision kinematics in the western external Alps. Tectonics, 33(6), 1055-1088, 2014.
331 Bergerat, F.: Stress fields in the European platform at the time of Africa-Eurasia collision. Tectonics
332 6, 99-132, 1987.
333 Bons, P. D., Elburg, M. A., and Gomez-Rivas, E.: A review of the formation of tectonic veins and
334 their microstructures. Journal of Structural Geology, 43, 33-62, 2012.
335 Carminati E., Aldega L., Smeraglia L., Scharf A., Mattern F., Albert R., and Gerdes A.: Tectonic
336 evolution of the Northern Oman Mountains, part of the Straits of Hormuz Syntaxis: new
337 structural and paleothermal analyses and U-Pb dating of synkinematic calcite. Tectonics 39,
338 e2019TC005936, 2020.
339 Craig, M. S., and Warvakai, K.: Structure of an active foreland fold and thrust belt, Papua New
340 Guinea. Australian Journal of Earth Sciences, 56(5), 719-738, 2009.
341 Craddock, J. P., Jackson, M., van der Pluijm, B. A., & Versical, R. T.: Regional shortening fabrics in
342 eastern North America: Far-field stress transmission from the Appalachian-Ouachita Orogenic
343 Belt. Tectonics, 12(1), 257-264, 1993.
344 Fagereng, Å., Remitti, F., and Sibson, R. H.: Shear veins observed within anisotropic fabric at high
345 angles to the maximum compressive stress. Nature Geoscience, 3(7), 482, 2010.
346 Ferril, D.A., Smart, K.J., Cawood, A.J., Morris, A.P.: The fold-thrust belt stress cycle: Superposition
347 of normal, strike-slip, and thrust faulting deformation regimes. Journal of Structural Geology
348 148, 104362, 2021.
349 Goodfellow, B. W., Viola, G., Bingen, B., Nuriel, P., and Kylander-Clark, A. R.: Paleocene faulting
350 in SE Sweden from U–Pb dating of slickenfiber calcite. Terra Nova, 29(5), 321-328, 2017.
351 Gratier, J. P., and Gamond, J. F.: Transition between seismic and aseismic deformation in the upper
352 crust. Geological Society, London, Special Publications, 54(1), 461-473, 1990.

353 Gratier, J.P., Thouvenot, F., Jenatton, L., Tourette, A., Doan, M.L., Renard, F.: Geological control of
354 the partitioning between seismic and aseismic sliding behaviours in active faults: evidence from
355 the Western Alps, France. Tectonophysics 600, 226-242, 2013.
356 Gruber, M.: Structural Investigations of the Western Swiss Molasse Basin - From 2D Seismic
357 Interpretaion to a 3D Geological Model. GeoFocus, 41, 190 pp, 2017.
358 Guillong, M., Wotzlaw, J., Looser, N., & Laurent, O. (2020). Evaluating the reliability of U–Pb laser
359 ablation inductively coupled plasma mass spectrometry (LA-ICP-MS) carbonate
360 geochronology: Matrix issues and a potential calcite validation reference material.
361 Geochronology, 2, 155–167. https://doi.org/10.5194/gchron-2-155-2020.
362 Hansman, R. J., Albert, R., Gerdes, A., and Ring, U.: Absolute ages of multiple generations of brittle
363 structures by U-Pb dating of calcite. Geology, 46(3), 207-210, 2018.
364 Hibsch, C., Jarrige, J. J., Cushing, E. M., and Mercier, J.: Palaeostress analysis, a contribution to the
365 understanding of basin tectonics and geodynamic evolution. Example of the Permian/Cenozoic
366 tectonics of Great Britain and geodynamic implications in western Europe. Tectonophysics,
367 252(1-4), 103-136, 1995.
368 Hoareau, G., Crognier, N., Lacroix, B., Aubourg, C., Roberts, N. M., Niemi, N., ... and Ruiz, I. S.:
369 Combination of Δ47 and U-Pb dating in tectonic calcite veins unravel the last pulses related to
370 the Pyrenean Shortening (Spain). Earth and Planetary Science Letters, 553, 116636, 2021.
371 Holland, M., and Urai, J. L.: Evolution of anastomosing crack–seal vein networks in limestones:
372 Insight from an exhumed high-pressure cell, Jabal Shams, Oman Mountains. Journal of
373 Structural Geology, 32(9), 1279-1290, 2010.
374 Homberg, C., Hu, J. C., Angelier, J., Bergerat, F., and Lacombe, O.: Characterization of stress
375 perturbations near major fault zones: insights from 2-D distinct-element numerical modelling
376 and field studies (Jura mountains). Journal of Structural Geology, 19(5), 703-718, 1997.

377 Homberg, C., Bergerat, F., Philippe, Y., Lacombe, O., and Angelier, J.: Structural inheritance and
378 Cenozoic stress fields in the Jura fold-and-thrust belt (France). Tectonophysics, 357(1-4), 137-
379 158, 2002.
380 Jordan, P.: Evidence for large-scale decoupling in the Triassic evaporites of Northern Switzerland:
381 an overview. Eclogae Geologicae Helvetiae, 85, 677–693, 1992.
382 Lacombe, O., Angelier, J., Laurent, P., Bergerat, F., and Tourneret, C.: Joint analyses of calcite twins
383 and fault slips as a key for deciphering polyphase tectonics: Burgundy as a case study.
384 Tectonophysics, 182(3-4), 279-300, 1990.
385 Lacombe, O., Angelier, J., Byrne, D., and Dupin, J. M.: Eocene-Oligocene tectonics and kinematics
386 of the Rhine-Saone continental transform zone (eastern France). Tectonics, 12(4), 874-888,
387 1993.
388 Lacombe, O., and Mouthereau, F.: What is the real front of orogens? The Pyrenean orogen as a case
389 study. Comptes Rendus de l'Academie des Sciences Series IIA Earth and Planetary Science,
390 329(12), 889-896, 1999.
391 Lacombe, O., & Mouthereau, F. (2002). Basement-involved shortening and deep detachment
392 tectonics in forelands of orogens: Insights from recent collision belts (Taiwan, Western Alps,
393 Pyrenees). *Tectonics*, *21*(4), 12-1.
394 Lacombe, O., and Obert, D.: Structural inheritance and cover deformation: Tertiary folding and
395 faulting in, the western Paris Basin. Comptes rendus de l'academie des sciences serie ii
396 fascicule a-sciences de la terre et des planetes, 330(11), 793-798, 2000.
397 Lacombe, O., Lavé, J., Roure, F. M., and Vergés, J. (Eds.).: Thrust belts and foreland basins: From
398 fold kinematics to hydrocarbon systems. Springer Science & Business Media, 2007.
399 Lacombe, O., and Bellahsen, N.: Thick-skinned tectonics and basement-involved fold–thrust belts:
400 insights from selected Cenozoic orogens. Geological Magazine, 153, 763-810, 2016.
401 Looser, N., Madritsch, H., Guillong, M., Laurent, O., Wohlwend, S., & Bernasconi, S. M. (2021).
402 Absolute age and temperature constraints on deformation along the basal décollement of the

403 Jura fold-and- thrust belt from carbonate U-Pb dating and clumped isotopes. Tectonics, 40,
404 e2020TC006439. https://doi. org/10.1029/2020TC006439
405 Madritsch, H., Schmid, S. M., and Fabbri, O.: Interactions between thin- and thick-skinned tectonics
406 at the northwestern front of the Jura fold-and-thrust belt (eastern France). Tectonics, 27, 1-31,
407 2008.
408 Mazurek, M., Davis, D. W., Madritsch, H., Rufer, D., Villa, I. et al. (2018). Veins in clay-rich
409 aquitards as records of deformation and fluid-flow events in northern Switzerland. Applied
410 Geochemistry, 95, 57-70, 2008.
411 Mazurek, M., Hurford, A. J., and Leu, W.: Unravelling the multi-stage burial history of the Swiss
412 Molasse Basin: integration of apatite fission track, vitrinite reflectance and biomarker
413 isomerisation analysis. Basin Research, 18, 27–50, 2006.
414 Mosar, J.: Present-day and future tectonic underplating in the western Swiss Alps: reconciliation of
415 basement/wrench-faulting and décollement folding of the Jura and Molasse basin in the Alpine
416 foreland. Earth and Planetary Science Letters, 173, 143-155, 1999.
417 Nuriel, P., Weinberger, R., Kylander-Clark, A. R. C., Hacker, B. R., and Craddock, J. P.: The onset
418 of the Dead Sea transform based on calcite age-strain analyses. Geology, 45(7), 587-590, 2017.
419 Parrish, R. R., Parrish, C. M., and Lasalle, S.: Vein calcite dating reveals Pyrenean orogen as cause
420 of Paleogene deformation in southern England. Journal of the Geological Society, 175(3), 425-
421 442, 2018.
422 Philippe, Y., Colletta, B., Deville, E., and Mascle, A.: The Jura fold-and-thrust belt: a kinematic
423 model based on map-balancing. Mémoires du Muséum national d'histoire naturelle, 170, 235-
424 261, 1996.
425 Pfiffner, O. A.: Geology of the Alps. Chichester: John Wiley & Son, 2014.
426 Rime, V., Sommaruga, A., Schori, M., and Mosar, J. : Tectonics of the Neuchâtel Jura Mountains:
427 insights from mapping and forward modelling. Swiss Journal of Geosciences, 112, 563-578,
428 2019.

Roberts, N. M., Drost, K., Horstwood, M. S., Condon, D. J., Chew, D., Drake, H., and Haslam, R.: Laser ablation inductively coupled plasma mass spectrometry (LA-ICP-MS) U-Pb carbonate geochronology: strategies, progress, and limitations. Geochronology, 2(1), 33-61, 2020.

Roberts, N. M., Žák, J., Vacek, F., and Sláma, J.: No more blind dates with calcite: Fluid-flow vs. fault-slip along the Očkov thrust, Prague Basin. Geoscience Frontiers, 12(4), 101143, 2021.

Sissingh, W.: Comparative Tertiary stratigraphy of the Rhine Graben, Bresse Graben and Molasse Basin: correlation of Alpine foreland events. Tectonophysics, 300, 249–28, 1998.

Smeraglia, L., Aldega, L., Billi, A., Carminati, E., Di Fiore, F., Gerdes, A., and Vignaroli, G.: Development of an Intrawedge Tectonic Mélange by Out-of-Sequence Thrusting, Buttressing, and Intraformational Rheological Contrast, Mt. Massico Ridge, Apennines, Italy. Tectonics, 38(4), 1223-1249, 2019.

Smeraglia, L., Fabbri, O., Choulet, F., Buatier, M., Boulvais, P., Bernasconi, S.M., and Castorina, F.: Syntectonic fluid flow and deformation mechanisms within the frontal thrust of foreland fold-and-thrust belt: Example from the Internal Jura, Eastern France. Tectonophysics, 778, https://doi.org/10.1016/j.tecto.2019.228178, 2020.

Sommaruga, A.: Geology of the Central Jura and the Molasse basin: New insight into an evaporite-based foreland fold and thrust belt. Mémoires de la Société Neuchâteloise de Sciences Naturelles, 12, pp. 176, 1997.

Sommaruga, A., Mosar, J., Schori, M., and Gruber, M.: The role of the Triassic evaporites underneath the North Alpine foreland. In Soto, J., Flinch, J., and Tari, G., (Ed.), Permo- Triassic salt provinces of Europe, North Africa and the Atlantic Margins: tectonics and hydrocarbon potential, chapter 22 (IV). Elsevier, 2017.

Thouvenot, F., Fréchet, J., Tapponnier, P., Thomas, J. C., Le Brun, B., Ménard, G., and Paul, A.: The ML 5.3 Epagny (French Alps) earthquake of 1996 July 15: a long-awaited event on the Vuache Fault. Geophysical Journal International, 135(3), 876-892, 1998.

454 Timar-Geng, Z., Fu¨genschuh, B., Wetzel, A., and Dresmann, H.: The low termperature thermal
455 history of northern Switzerland as revealed by fission track analysis and inverse thermal
456 modelling. Eclogae Geologicae Helvetiae, 99, 255–270, 2006.
457 Twiss, R. J., and Moores, E. M.: Structural geology. Macmillan, 1992.
458 Urai, J. L., Williams, P. F., and Van Roermund, H. L. M.: Kinematics of crystal growth in syntectonic
459 fibrous veins. Journal of Structural Geology, 13(7), 823-836, 1991.
460 Ustaszewski, K., and Schmid, S. M.: Control of preexisting faults on geometry and kinematics in the
461 northernmost part of the Jura fold-and-thrust belt. Tectonics, 25, 1-26, 2006.
462 Van der Pluijm, B. A., Hall, C. M., Vrolijk, P. J., Pevear, D. R., and Covey, M. C.: The dating of
463 shallow faults in the Earth's crust. Nature, 412(6843), 172-175, 2001.
464 Vergés, J., Muñoz, J. A., and Martínez, A.: South Pyrenean fold and thrust belt: The role of foreland
465 evaporitic levels in thrust geometry. In Thrust tectonics, 255-264. Springer, Dordrecht, 1992.
466 Von Hagke, C., Cederbom, C. E., Oncken, O., Stöckli, D. F., Rahn, M. K., and Schlunegger, F.:
467 Linking the northern Alps with their foreland: The latest exhumation history resolved by low-
468 temperature thermochronology. Tectonics, 31(5), 2012.
469 Von Hagke, C., Oncken, O., Ortner, H., Cederbom, C. E., and Aichholzer, S.: Late Miocene to present
470 deformation and erosion of the Central Alps—Evidence for steady state mountain building from
471 thermokinematic data. Tectonophysics, 632, 250-260, 2014.
472 Vrolijk, P., Pevear, D., Covey, M., and LaRiviere, A.: Fault gouge dating: history and evolution. Clay
473 Minerals, 53(3), 305-324, 2018.
474 Woodcock, N. H., Miller, A. V. M., & Woodhouse, C. D.: Chaotic breccia zones on the Pembroke
475 Peninsula, south Wales: Evidence for collapse into voids along dilational faults. Journal of
476 Structural Geology, 69, 91-107, 2014.
477